

We are IntechOpen, the world's leading publisher of Open Access books Built by scientists, for scientists

6,900

Open access books available

186,000

International authors and editors

200M

Downloads

Our authors are among the

154

Countries delivered to

TOP 1%

most cited scientists

12.2%

Contributors from top 500 universities



WEB OF SCIENCE™

Selection of our books indexed in the Book Citation Index
in Web of Science™ Core Collection (BKCI)

Interested in publishing with us?
Contact book.department@intechopen.com

Numbers displayed above are based on latest data collected.
For more information visit www.intechopen.com



Hyaluronic Acid Derivatives for Targeted Cancer Therapy

Nilkamal Pramanik and Sameer Kumar Jagirdar

Abstract

Targeted therapeutics are considered next generation cancer therapy because they overcome many limitations of traditional chemotherapy. Cancerous cells may be targeted by various hyaluronic acid modified nanovehicles that kill these cells. Particularly, hyaluronic acid and its derivatives bind with high affinity to cell surface protein, CD44 enriched tumor cells. Moreover, these molecules have the added advantage of being biocompatible and biodegradable, and may be conjugated with a variety of drugs and drug carriers for developing various formulations as anti-cancer therapies such as nanogels, self-assembled and metallic nanoparticulates. In this chapter, we have covered various aspects of hyaluronic acid-modified delivery systems including strategies for synthesis, characterization, and biocompatibility. Next, the use of hyaluronic acid-modified systems as anti-cancer therapies is discussed. Finally, the delivery of small molecules, and other pharmaceutical agents are also elaborated in this chapter.

Keywords: Hyaluronic Acid, Nano-particulates, Immunogenicity, Biodegradation, Tumor Targeted delivery

1. Introduction

Nanoparticles have gained increased attention in the context of cancer therapy; however, the major challenge of targeting particles specifically to cancerous cells remains. Targeted delivery systems comprising cell-targeting ligands such as antibodies, peptides, folic acid, and various biomolecules have been developed to ensure tumor-specific delivery. One such targeting ligand is hyaluronic acid (HA).

HA, a glycosaminoglycan (GAG), is a natural polysaccharide present in the extracellular matrix of various soft connective tissues such as the vitreous humor, dermis of the skin, hyaline cartilage, and synovial fluid of the body. It is water-soluble, viscoelastic, biodegradable, biocompatible, and non-immunogenic [1–4]. HA is a polyanionic mucopolysaccharide consisting of β -1,3 and β -1,4 glycosidic bonds between repeating units of D-glucuronic acid and N-acetyl-D-glucosamine [5].

As an intrinsic part of the ECM, HA participates in different biological functions of the cell, including signal transduction, vascularization, cell migration, and tissue remodeling as schematically represented in **Figure 1**. Additionally, the presence of modifiable hydrophilic functional groups—hydroxyl, carboxyl, and N-acetyl increases its potential as an adaptable system for the delivery of proteins, nucleic acids, and anti-cancer agents by grafting or modification with different nanoparticles. Based on cellular interaction studies, HA has emerged as a tumor-targeting agent in cancer therapy. It exhibits a

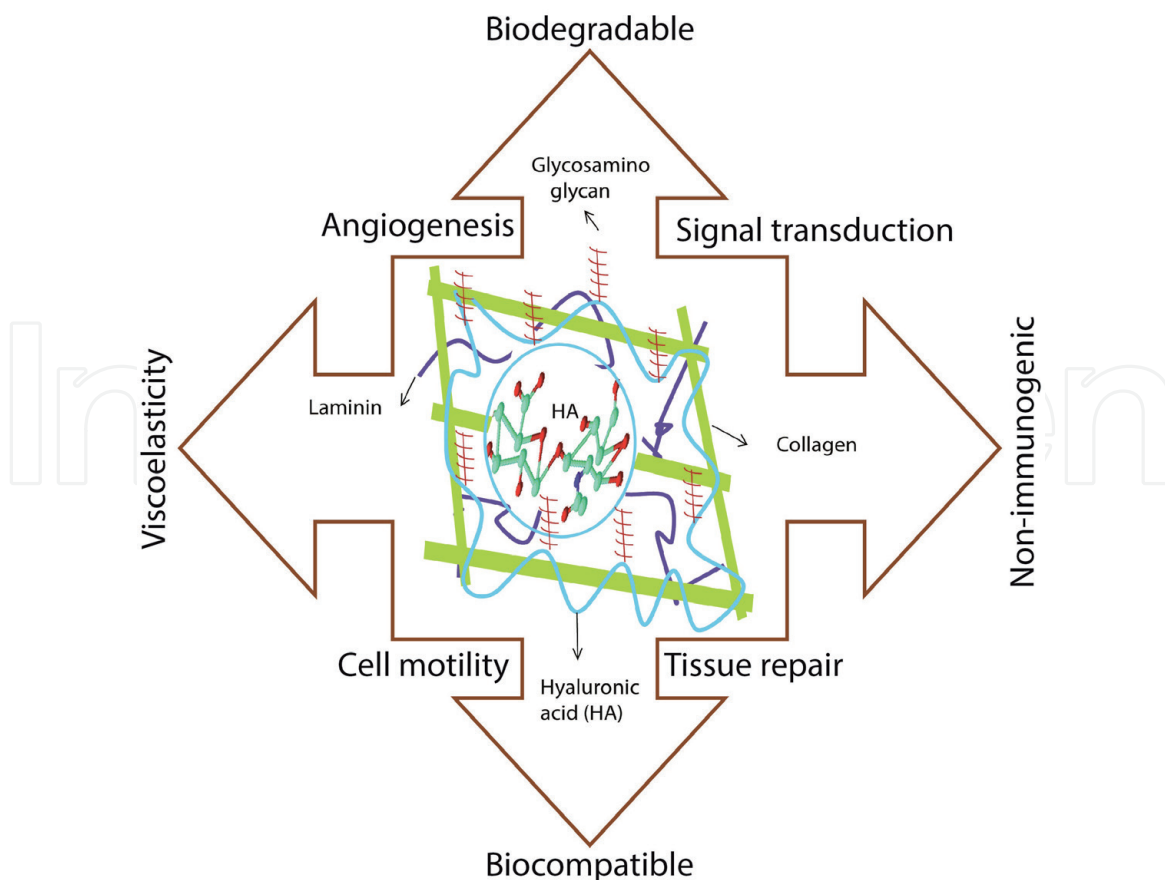


Figure 1. Schematic representation of physico-chemical properties and functions of hyaluronic acid (HA) in the native tissue environment.

high binding affinity towards the CD44 cluster [6], which is over-expressed in numerous malignant cancer cells [7–9].

Considering its hierarchical structure and potential as a targeting agent, HA can be modified using small biomolecules [10], nanotubes [11], or different types of metal and non-metal nanoparticles [12] in various formulations. HA modified particles are effectively ingested by cells, and HA is enzymatically degraded intracellularly [13], resulting in the delivery of only the particles and their cargo inside the cell.

This chapter covers various aspects of HA-modified delivery systems, including strategies for synthesis, characterization, and biocompatibility. Furthermore, the characteristics of different delivery systems such as nanogel, micelle, liposome, and metallic or non-metallic nano-particulates are discussed. The mechanism underlying the delivery of small molecules, nucleic acids, and other pharmaceutical agents (*in vitro*, *in vivo*, or clinical applicability) are also presented in this chapter.

2. Hyaluronic acid—a primer

HA was discovered in 1934 when scientists Karl Meyer and John Palmer isolated a new kind of polysaccharide from bovine vitreous humor, which was later termed as hyaluronan [14]. Hyaluronic acid is a polysaccharide composed of repeating units of β -1,3-N-acetyl-D-glucosamine and β -1,4-D-glucuronic acid linked by β -1,3 and β -1,4 glycosidic bonds. It is a component of the extracellular matrix and mediates various cellular functions. HA is a ligand for the cell surface receptor CD44. CD44

is a transmembrane protein that is typically expressed by a number of cells, but is over-expressed in different types of metastatic tumor cells, including those of brain, breast, prostate, colon, bladder, and head and neck cancers [7–9, 15–17]. It has a significant role in cell proliferation, migration, metastasis, and cell–cell and cell-matrix signal transduction [18].

2.1 Synthesis

Hyaluronic acid is usually obtained from different biological sources. The microbial synthesis pathway is preferred as it is cost-effective and an environmentally benign process. The gram-positive bacterium, *Streptococcus zooepidemicus* is used for large-scale production of HA via a fermentative pathway as shown in **Figure 2(A)** [19]. The biosynthetic pathway of HA is as follows: initially, glucose-6-phosphate is converted to uridine diphosphate glucose (UDP-glucose) in the presence of α -phosphoglucosomutase and UDP-glucose dehydrogenase followed by UDP-glucose dehydrogenase assisted oxidation into UDP-glucuronic acid. Next, an amide group is transferred from glutamine-fructose-6-phosphate to fructose-6-phosphate, followed by rearrangement of the phosphate leading to the formation of glucosamine-1-phosphate. Subsequently, acetylation and conjugation of UTP to glucosamine-1-phosphate generates the second precursor of HA. In the final step, hyaluronan synthase polymerizes the two precursors to produce HA, which is presented as an extracellular capsule as confirmed by electron microscopy (see **Figure 2(B)**) [20]. However, the pathogenicity of the bacterium limits its use for mass production of HA and therefore, several recombinant strains such as *Agrobacterium* sp. ATCC 31749 and recombinant *Escherichia coli* have been adapted as an alternative source of HA production [21, 22].

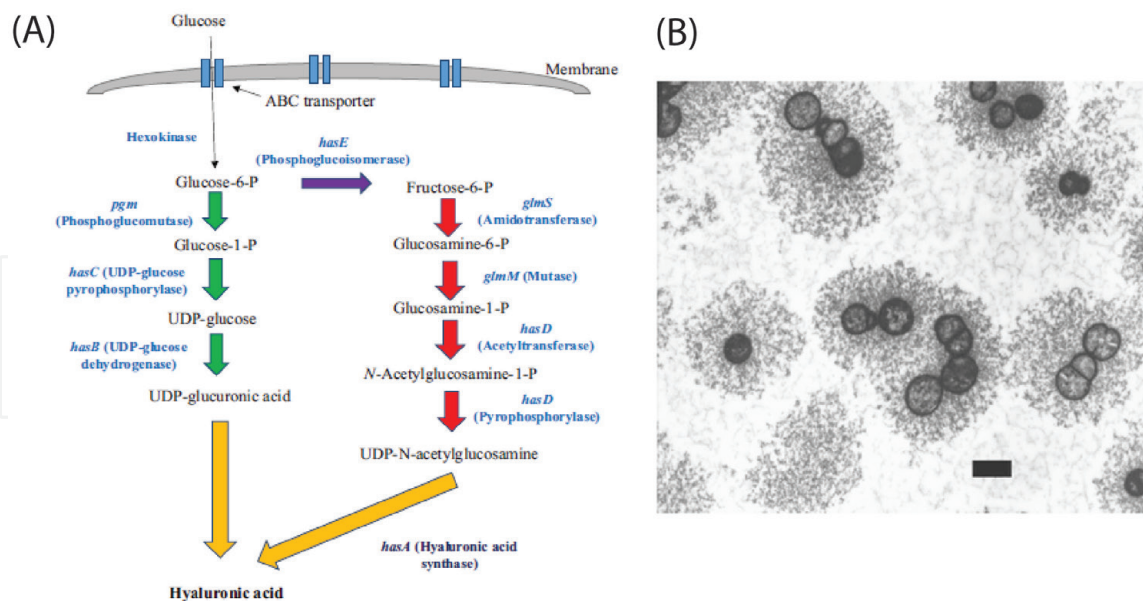


Figure 2. (A) Hyaluronic acid biosynthetic pathway in *S. zooepidemicus*. Glucose is first converted to glucose-6-phosphate by hexokinase which then enters one of two distinct pathways to form UDP-glucuronic acid (*pgm*, *hasC* and *hasB*) or UDP-N-acetylglucosamine (*hasE*, *glmS*, *glmM* and *hasD*). These precursors are subsequently bound together via the action of hyaluronic acid synthase or HAVE (encoded by *hasA* in *S. zooepidemicus*) to form hyaluronic acid. [Ref. [19], reproduced with permission from publishing authority]. (B) Electron micrograph section of *Streptococcus equi* subsp. *Zooepidemicus* (*S. zooepidemicus*) cells obtained from the late exponential phase of an aerated bioreactor culture. Thin sections were stained with uranyl acetate and lead citrate and examined with a Jeol JEM-1010 transmission electron microscope at an accelerating voltage of 80 kV. Bar 1 μm . [Ref. [20], reproduced with permission from publishing authority].

2.2 Properties and uses

As mentioned previously, HA is a polymer. The physiochemical properties such as rheology and viscoelasticity of the polymer depend on the length of HA. Previous studies have demonstrated that higher molecular weight HA has better wound healing properties and is more effective for orthopedic treatment whereas low molecular weight HA has a prominent role in angiogenesis and is an effective immuno-stimulant [23]. A variety of HA oligosaccharides have been synthesized chemically, ranging from disaccharides to hexasaccharides to improve biomedical availability and use. Lu et al. synthesized HA decasaccharides using a chemoselective glycosylation pathway [24]. Commercially available D-glucose and D-glucosamine hydrochloride are chemically connected in the presence of an activator to generate various HA-derivatives [25].

3. Applications in cancer therapy

On the basis of their physiochemical properties, different HA-based nano-formulations have been investigated for their therapeutic application in tumor-therapy. HA conjugated drugs, polymers, and lipids may self-assemble in aqueous solvents, and this property has been used to synthesize a number of self-assembled nano-particulates that are either made of the drug or contain the drug.

3.1 Drug-HA conjugates

Direct conjugation of drug molecules with HA results in the development of systems that are not only capable of targeting but improve solubility as well as blood circulation times of the drug itself. Some of the methods to synthesize drug-HA nanoparticles are summarized in **Figure 3**, and below, we discuss a few examples of the use of HA in developing new anti-cancer therapeutics.

The first example, presented in **Figure 3(A)**, involves the conjugation of HA with succinic anhydride derived paclitaxel (2-succPTX, a tubulin inhibitor) using glutathione (GSH) sensitive cystamine (or non-sensitive adipic dihydrazide) as a cross-linker. The resultant self-assembled nanoparticles formed were analyzed using ^1H nuclear magnetic resonance (NMR), Fourier-transform infrared spectroscopy (FTIR), and UV-visible spectroscopy. Transmission electron microscopy (TEM) and atomic force microscopy (AFM) analysis demonstrated the presence of spherical shaped nanoparticles of diameter 150 nm. The nanoparticles accurately targeted cancer cells with significant anti-tumor efficacy both *in vitro* and *in vivo* as compared to free PTX [26]. Along similar lines, another HA-PTX nanovehicle showed excellent results in reducing tumor size with the increase of survival rate in an *in vivo* mouse xenograft model bearing ovarian cancer cells [27]. A recent development in this area was to improve the loading of PTX in these self-assembled nanoparticles through the use of dimethylsulfoxide (DMSO) and polyethylene glycol (PEG) in the organic phase. This nano-system was suggested to have a 10–20% increase in PTX loading, and as a result, had significant anti-tumor activity against the RT-4 and RT-112/84 bladder carcinoma cell-lines [28].

The second example is the synthesis of a HA-doxorubicin (DOX) based self-assembled pro-drug that formed spherical core-shell nanostructures (**Figure 3(B)**) of 180–200 nm diameter. It displayed good biocompatibility and pH-responsive controlled Dox release in a cervical cancer model and exhibited excellent tumor inhibitory effects [29]. An ion-pairing based Dox-HA nano-assembled structure

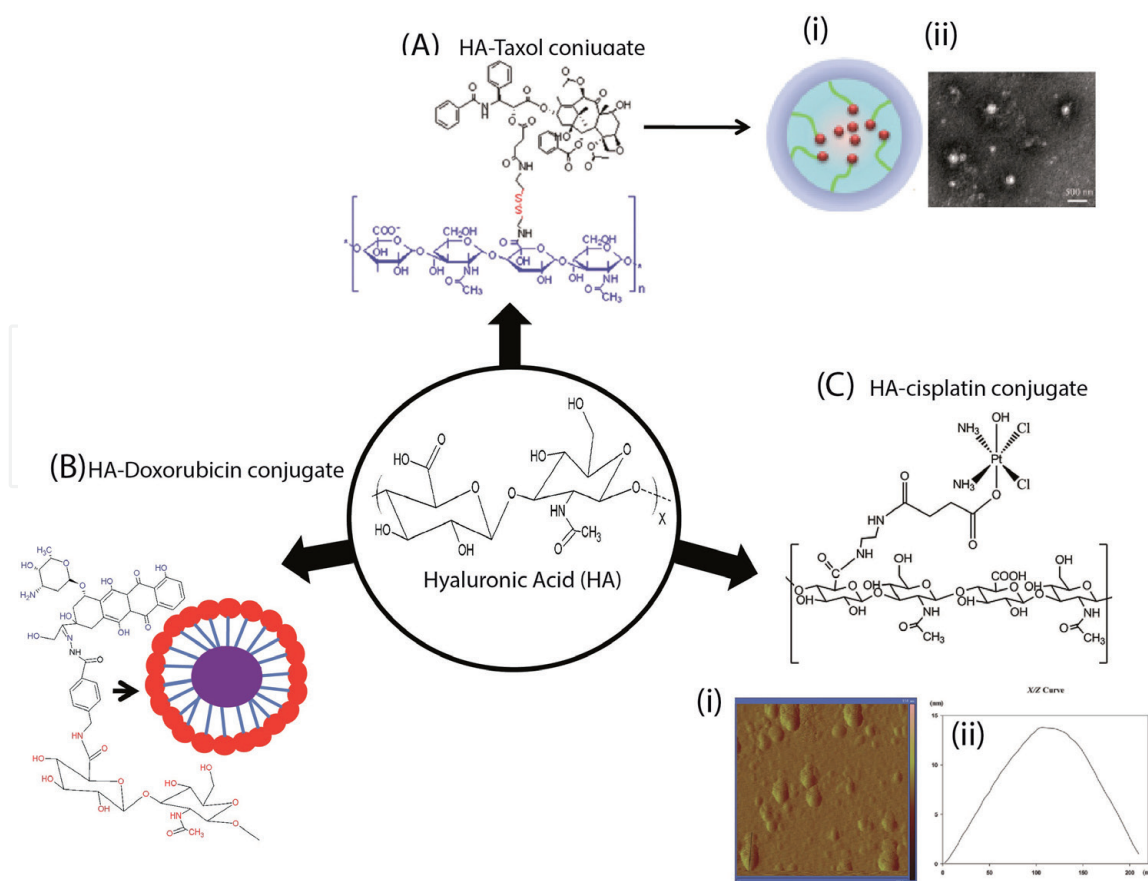


Figure 3.

(A) Synthesis of 2'-succinylated paclitaxel (PTX) and cystamine (ss) modified hyaluronic acid (HA)-g-paclitaxel (PTX) [HA-ss-PTX] through two consecutive pathways. Initially, PTX was functionalized with succinic anhydride to obtain an active free carboxylic acid group which was further grafted with HA in the presence of cystamine as a cross-linker using EDAC. HCl and NHS reaction chemistry mechanism. [A(i&ii)] illustrate the schematic and TEM images of HA-PTX based self-assembled structure. [Ref. [26], adapted with permission from publishing authority]. (B) Schematic presentation of the synthesis of amide methyl 4 (aminomethyl) benzoate crosslinked with self-assembled HA-doxorubicin graft. (C) Synthesis of 2, 7-succinylated cisplatin [2, 7-Succ-Pt(IV)] followed by ethylene diamine (EDA) mediated conjugation with HA using EDAC. HCl and NHS reaction chemistry to form HA-EDA-Pt(IV) pro-drug. [C(i&ii)] AFM images of HA-EDA-Pt(IV) nanoconjugate at an optimal dilution ratio, indicating the formation of microspheres with an average diameter of 200 nm. [Ref. [31], adapted with permission from publishing authority].

with a liposomal delivery system displayed sustained intracellular release of Dox in CD44+ cancer cells with enhanced therapeutic efficacy in a mouse model [30].

The third and final example is the conjugation of HA with cisplatin. Cisplatin is an anti-cancer drug that causes adverse side-effects. Increasing cancer cell-specific intracellular delivery of cisplatin may reduce side effects, which might be possible by conjugating HA onto the drug. Ling et al. have demonstrated the synthesis of HA conjugated cisplatin using N-(3-dimethylaminopropyl)-N'-ethylcarbodiimide hydrochloride. The synthesized pro-drug was verified using ¹HNMR, ¹³C NMR, FT-NIR, AFM, and DSC analysis. The prepared pro-drug was spherical (**Figure 3(C)**) and showed CD44 mediated endocytosis with negligible stimulation to blood vessels. Systemic toxicity studies indicated that the drug was safe and actively delivered cisplatin to kill tumor cells with reduced adverse effect on healthy cells [31].

3.2 Drug loaded HA based nanoparticles

HA may also be conjugated with lipids and other small molecules, which also self-assemble to form particulates that may be used to encapsulate drugs. One example of such a system is deoxycholic acid conjugated with HA, which results

in the formation of micelles that may, in turn, be loaded with drug molecules (**Figure 4(A)**). In the specific study presented in this figure, Huo and colleagues showed that the average hydrodynamic size and colloidal stability in terms of ‘zeta potential’ of the resultant micelle was 120 nm and 36 mV, respectively. These particles were capable of releasing taxol (the drug here) into the cytoplasm of cancer cells, causing tumor apoptosis, with a minimum adverse effect on healthy cells [32]. In another study, cholesterol coupled HA was employed as the amphiphilic molecule that self-assembles into nanoparticles that encapsulate both the anti-cancer drug Dox and magnetic nanoparticles (**Figure 4(B)**). This multifunctional delivery system exhibited high cytotoxicity and cellular uptake against several cancer cell lines such as HeLa, HepG2, and MCF7 [33].

Utilizing HA-molecule conjugated self-assembled nanovehicles for drug loading enables the development of combinatorial therapeutic approaches. As an example of such an approach, the photo-sensitizer, Ce6, has been coupled with HA to form a self-aggregated system that is capable of delivering therapeutic drugs. Such a system was used in a human colon xenograft and displayed a significant anti-tumor effect

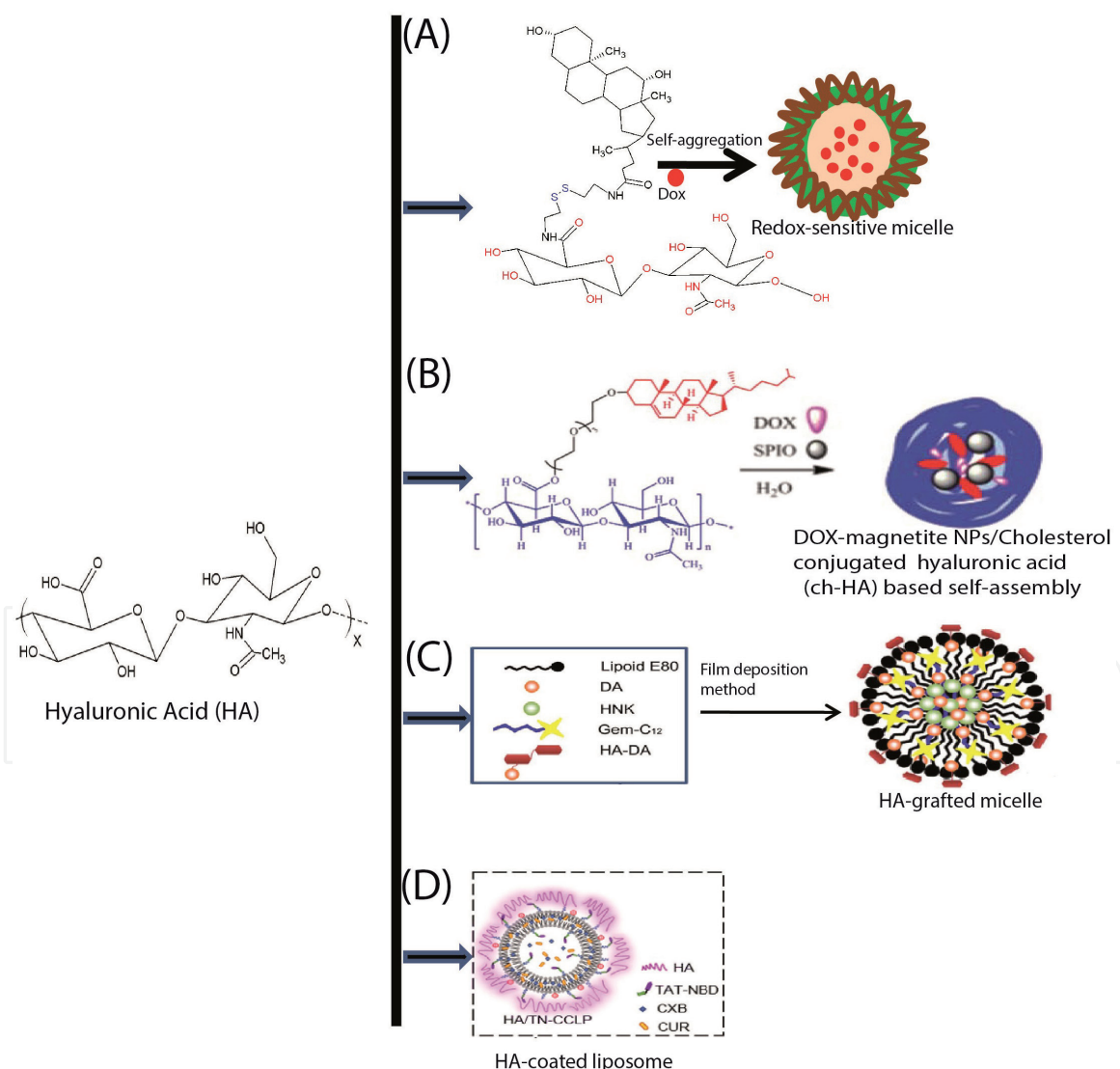


Figure 4.

(A) Schematic illustration of cystamine (ss) cross-linked deoxycholic acid (DOCA) conjugated hyaluronic acid (HA) [HA-ss-DOCA conjugate] nanoparticles. (B) Schematic illustration of the synthesis of cholesterol-conjugated HA (ch-HA) and the formation of DOX/SPIO loaded ch-HA micelles. [Ref. [33], adapted with the permission from publishing authority]. (C) Schematic illustration of the preparation of HA-grafted micelles (HA-M) [Ref. [36], reproduced with permission from publishing authority]. (D) Preparation of HA/TN-CCLP and other liposomes. [Ref. [37], adapted with permission from publishing authority].

in a mouse model [34, 35]. In the case of brain tumor therapy, the delivery of chemotherapeutic agents is hindered by the sophisticated blood–brain barrier (BBB) [36], and such combinatorial therapeutics could be beneficial for hard-to-treat cancers such as glioblastoma multiforme (GBM). Combinatorial chemotherapy strategies based on lauroyl-gemcitabine, honokiol (HNK), and HA grafted micelle formulations (**Figure 4(C)**) were shown to significantly suppress GBM in an *in vivo* xenograft model [36]. Similarly, Liposomes composed of TAT-NBD (TN, a 22 amino acid cell-penetrating peptide) modified HA, encapsulating celecoxib (CXB) and curcumin (CUR) (HA/TN-CCLP) (**Figure 4(D)**) were reported to block nuclear factor- κ B (NF- κ B) and signal transducer and activator of transcription 3 (STAT3) signaling pathways, potentially inhibiting tumor growth and metastasis by improving infiltration of inflammatory cells [37].

3.3 Gel formulations

One of the major advantages of using HA is its ability to be used in diverse forms. As HA is an extracellular matrix protein, it may also be used to form hydrogels by itself or in combination with other polysaccharides. Injectable polymeric hydrogels have made a significant contribution to active targeted delivery of chemotherapeutic agents as the 3-dimensional porous environment allows for pH or thermo-sensitive controlled intracellular release of cargo. A HA modified chitosan grafted poly-N-isopropylacrylamide hydrogel was reported to have the loading capacity of Dox/folic acid-g-graphene sheets with high killing efficacy against MCF7 breast cancer cells. An *in vivo* study also demonstrated delivery of anti-tumor agents using the same system [38].

Interferon α -2a (IFN α -2a) loaded HA–tyramine hydrogels have also been shown to have anti-tumor effects, while native IFN α -2a injection did not show any anti-cancer effects. This was due to the controlled release of IFN α -2a from the hydrogel network [39]. Such gels may also be developed as nano-formulations, as demonstrated by Jaya Kumar and colleagues who showed that a redox-sensitive Dox loaded chitin-cystamine-HA nanogel may be used to specifically kill CD44+ HT-29 cells [40].

3.4 Graphene oxide (GO) based formulations

In the past couple of decades, carbonaceous compounds have gained significant attention in cancer therapy due to their large surface area and bio-sensing, bio-imaging, cellular probing, and drug carrier abilities. Owing to its 2D structure, biocompatibility, and water-dispersion features, graphene oxide (GO) and its HA conjugate have been investigated as anti-cancer drug delivery platforms. Three specific examples are discussed here.

First is the development of HA and Arg-Gly-Asp (RGD) peptide coated graphene oxide as a nano-carrier for Dox. Raman spectroscopic analysis revealed two strong peaks at 1350 cm^{-1} and 1550 cm^{-1} due to the presence of D and G bands in exfoliated graphene oxide, as shown in **Figure 5(A)**, which was further confirmed by TEM. The nano-carrier was composed of a single transparent layer with a gauze-like lid layer. It exhibited high Dox loading capacity and excellent cytotoxicity when tested on an ovarian cancer cell line, SKOV-3. It was also found to be biocompatible when tested on a healthy human cell line, HOSEpiC [41].

The second is the development of a redox-sensitive near-infrared (NIR) controlled system consisting of both HA and GO. Yin et al. demonstrated (**Figure 5(B)**) that a Dox/HA-cystamine-GO nano-carrier displays selective targeting and glutathione responsive release of Dox in the cytosol without any collateral damage to healthy

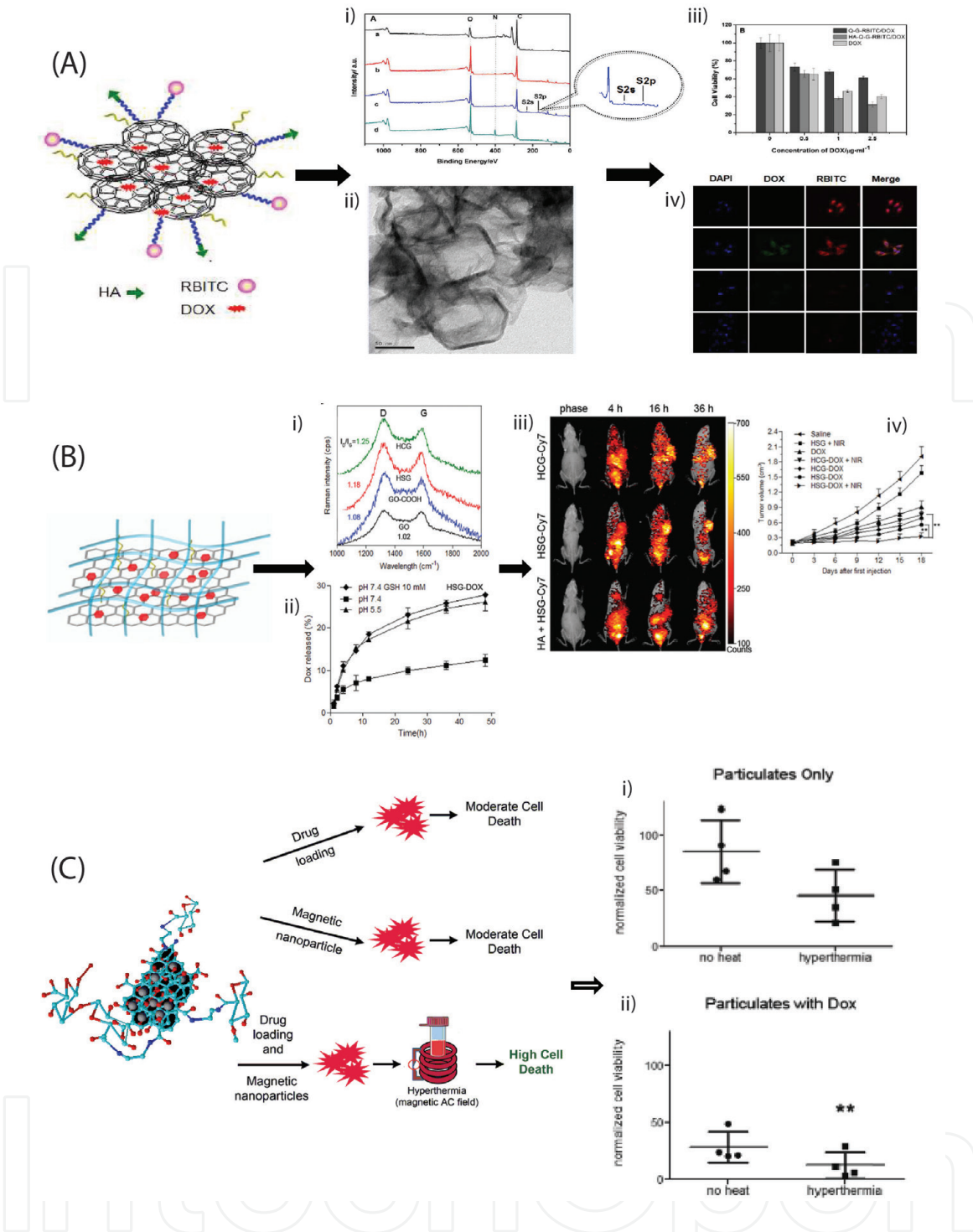


Figure 5.

(A) Schematic illustration of the preparation and characterization of RBITC labeled Q-graphene (HA-Q-G-RBITC)/DOX nanoparticles and HA-mediated endocytosis. (i) XPS analysis of Q-graphene (a), Q-graphene-COOH (b), Sulf-Q-graphene (c), and PEG Q-graphene (d). (ii) TEM image of Q-graphene. (iii) cytotoxic effects of Q-G-RBITC/DOX, HA-Q-G-RBITC/DOX, and DOX against A549 cells with increasing DOX concentration. The error bar represents standard deviation ($n = 5$). (iv) CLSM images of A549 cells incubated with (A) HA-Q-G-RBITC, (B) HAQ-G-RBITC/DOX, or (C) Q-G-RBITC/DOX for 5 h. (D) MRC-5 cells incubated with HA-Q-G-RBITC/DOX for 5 h. [Ref. [41], reproduced with permission from publishing authority]. (B) Synthesis of HSG-DOX nanosheets. (i) Raman absorption spectra of HCG, HSG, GO-COOH, and GO. (ii) In vitro DOX release from HSG-DOX after incubation with glutathione at 37°C. (iii) In vivo fluorescent imaging of MDA-MB-231 tumor-bearing nude mice at 4, 16, and 36 h after intravenous injection of Cy7-labeled HSG-DOX and HCG-DOX nanosheets with or without pre-injection of free HA at HSG/HCG dose of 5 mg/kg. (iv) tumor growth curves after intravenous injection of different formulations at a DOX dose of 5 mg/kg. $**P < 0.01$. [Ref. [12], reproduced with permission from publishing authority]. (C) Synthesis of dox loaded magnetite nanoparticles/GO-HA. Cytotoxicity induced by combination of drug treatment and hyperthermia. GO-HA-iron oxide particulates (i) without or (ii) with dox were cultured with MDA-MB-231 cells and exposed to magnetic fields, and cell viability was measured. Cell viability measurements are normalized to control cultures of cells in the absence of particulates, drugs, and hyperthermia. Paired Student's t -test was performed to compare hyperthermia treatment to their respective no-heat controls. $**p < 0.01$. [Ref. [43], adapted with permission from publishing authority].

cells. As compared to free Dox, the NIR irradiated nanosystem exhibited enhanced cytotoxicity in a xenograft tumor model [12]. A similar cytotoxic effect was observed when HiLyte 647 loaded nano GO-HA was used to treat melanoma. Photo-thermal treatment resulted in the complete ablation of tumor tissue without any further tumorigenesis [42].

The third example is our own work on a formulation containing magnetic nanoparticle decorated GO-HA, which was evaluated for magnetothermal and CD44 (+) positive breast cancer targeted cancer therapy. As shown in **Figure 5(C)**, the nanoplatform can be loaded with various types of chemotherapeutic agents such as Dox and Ptx. Furthermore, the study revealed that the nanoplatform had significant anti-tumor activity under magnetic hyperthermia in the MDA MB231 cell line. These nanovehicles provide a versatile platform for next-generation cancer therapy [43].

3.5 Other carriers

Owing to their high stability, biocompatibility, and tunable porous architecture, mesoporous silica nanoparticles (MSNPs) have been used as multifunctional tumor-targeting nano-carriers. Dox loaded HA modified MSNPs have been developed and tested against HCT-116 cells, as shown in **Figure 6(A)**. As part of the morphological analysis, TEM revealed spherical nanoparticles organized as a hexagonally packed mesoporous structure with a mean particle size of 70–100 nm. Surface modification of the MSNPs was confirmed by ^{13}C NMR analysis. Strong absorption peaks at 43, 22, and 10 ppm and broad peaks at 70–180 ppm confirmed the presence of the methylene carbon in NH_2 -MSNPs and the anomeric carbon in HA, respectively. Compared to free Dox and Dox loaded MSNPs, Dox-HA-MSNPs exhibited a significantly greater anti-proliferative effect because of better CD44 mediated uptake of HA modified nanoparticles at physiological pH [44].

A similar approach was used to fabricate mesoporous silica nanoparticles, post-functionalized with PEG-PDS-NH₂ [poly(poly(ethyleneglycol) methacrylate-co-pyridyldithioethyl methacrylate-co-2 aminoethylmethacrylate)], followed by HA decoration for selective targeting. As shown in **Figure 6(B)**, Dox loaded nanoparticles demonstrated clathrin and macropinocytosis-mediated cellular uptake with the killing of CD44 positive HeLa cells [45].

Gold nanoparticles (AuNPs) in cancer therapy have dual functionality due to the presence of a bioactive surface, contrast ability, and photodynamic features. Kang et al. developed HA conjugated pheophorbide-A coated AuNPs (**Figure 6(C)**) that had excellent colloidal stability and photoactivity in the intracellular environment [46]. Electron microscopy analysis of the hybrid nanomaterial revealed spherical nanoparticles with a mean diameter of 70–80 nm, whereas native gold nanoparticles had a mean diameter of 10–15 nm. The increase in size is attributed to the surface coating of the AuNPs. Active targeting was observed 48 h post-injection of PheoA-HA/AuNPs as indicated by bright fluorescence intensity at the tumor site rather than elsewhere, suggesting CD44 receptor-mediated accumulation of nanoparticles with minimum adverse effects on healthy tissues. *In vivo* study of administration of PheoA-HA/AuNPs revealed their excellent anti-tumor efficacy with 3-fold to 5-fold decrease in tumor size compared to free PheoA, saline, and AuNPs. In another study, Wang et al. synthesized $\{(\text{Au}0)100\text{G}5.\text{NH}_2\text{-FI-DOTA}(\text{Mn})\text{-HA}$, where DOTA-1, 4, 7, 10-tetraazacyclododecane-1, 4, 7, 10-tetraacetic acid} NPs which facilitated selective internalization of dendrimers in tumor cells whose imaging capability is presented in **Figure 6(D)** [47].

Super-paramagnetic iron oxide nanoparticles have gained tremendous attention in targeted cancer therapy due to their diverse properties, including

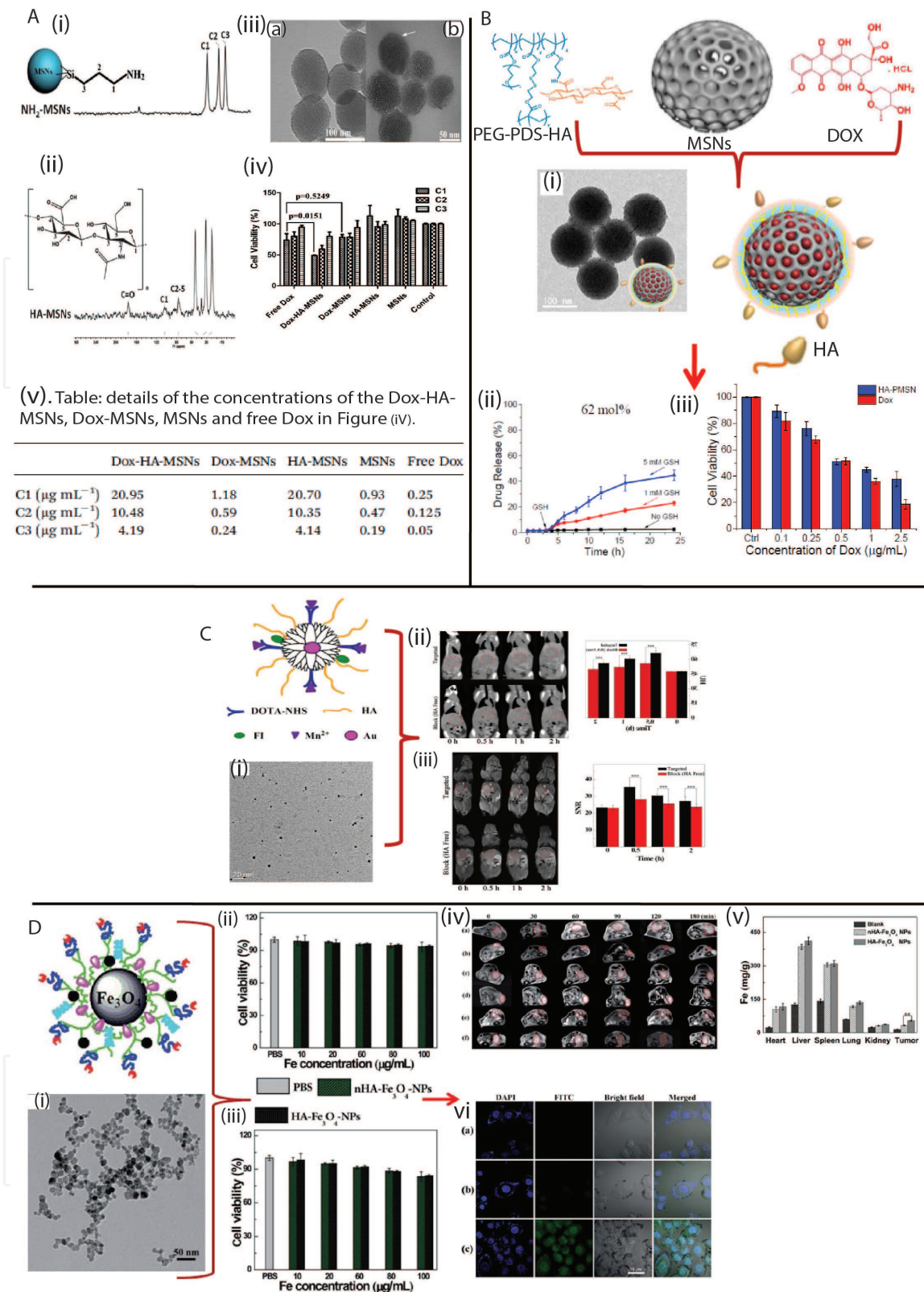


Figure 6. (A) Synthesis of different hyaluronic acid (HA) modified metal nano formulations for targeted cancer therapy. [A(i&ii)]. ^{13}C NMR spectra of NH_2 -MSNs and HA-MSNs. [iii(a&b)]. TEM images of MSNs and (iv) HA-MSNs. (D) Cytotoxicity of free dox, dox-HA-MSNs, dox-MSNs, HA-MSNs and MSNs against HCT-116 cells at different concentrations C1, C2 and C3 (for details, see table v). [Ref. [44], adapted with permission from publishing authority]. (B) Schematic illustration of efficient mesoporous nanoparticle-mediated DDS using noncovalent polymer gatekeepers and HA conjugation for targeting capability. (i) TEM images of HA-PMSNs, (ii) cumulative dox release profiles of 62 Mol% crosslinked PMSNs with (1 and 5 mM) and without GSH. (iii) cell viability analysis of HA-PMSNs CD44-positive in HeLa cells. [Ref. [45], adapted with permission from publishing authority]. (C) Schematic representation of the synthesis of $\{(Au)_0\}_{100}G_5.NH_2-FI-DOTA (Mn)-HA\}$ NPs. (i) TEM image of the $\{(Au)_0\}_{100}G_5.NH_2-FI-DOTA (Mn)-HA\}$ NPs. The scale bar in each panel measures 20 nm. (ii) In vivo CT images of orthotopic liver tumors at different times after a 0.3-mL intravenous injection of a $\{(Au)_0\}_{100}G_5.NH_2-FI-DOTA (Mn)-HA\}$ NP solution (0.3 mL

in PBS, $[Au] = 120 \text{ mM}$). (iii) *In vivo* MR images of orthotopic liver tumors at different times after an intravenous injection of 0.3 mL of a $\{(Au_0)_{100}G_5.NH_2-FI-DOTA (Mn)-HA\}$ NP (300 $\mu\text{g Mn}$) solution in PBS. [Ref. [47], adapted the permission from publishing authority]. (D) Synthesis of HA-modified magnetite nanoparticles (HA- Fe_3O_4 NPs) (i) TEM micrographs of HA- Fe_3O_4 NPs. The viability of MIA PaCa-2 cells after treated with PBS, nHA- Fe_3O_4 NP and HA- Fe_3O_4 NPs at the different Fe concentrations for 24 h (ii) or 48 h (iii) at 37 °C by the CCK-8 assay (iv) *In vivo* transverse T2 MR images of tumors after intravenous injection of the nHA- Fe_3O_4 NP ((a) 7 days; (c) 14 days; (e) 21 days) and HA- Fe_3O_4 NPs ((b) 7 days; (d) 14 days; (f) 21 days) ($[Fe] 1 \text{ mg/mL}$, in 200 mL saline) at different time points post i.v.-injection. (v) *In vivo* biodistribution of hearts, livers, spleens, lungs, kidneys, and tumors 24 h post intravenous injection of the nHA- Fe_3O_4 NP and HA- Fe_3O_4 NPs (600 mg Fe, in 0.3 mL PBS). (vi) The ability of MIA PaCa-2 cells to uptake PBS (a), nHA- Fe_3O_4 NP (b) and HA- Fe_3O_4 NPs (c) ($[Fe] 50 \text{ mg/mL}$) 4 hours after treatment, MIA PaCa-2 cells treated with PBS were used as control, scale bar $\frac{1}{4} 10 \text{ mm}$. [Ref. [48], adapted with permission from publishing authority].

biocompatibility, enabling their use as a contrast agent for MRI and in magneto-thermal therapy. Moreover, their tendency for aggregation in an aqueous medium is avoided by coating with active biopolymers and cancer-targeting agents. For example, HA modified and fluorescein isothiocyanate decorated iron nanoparticles may be utilized as an efficient probe for targeted MRI assisted cancer therapy, as shown in **Figure 6(E)** [48].

Another use of these particulates could be targeted brain tumor therapy, and a specific example is the development of HA-polyethylene glycol stabilized magnetite nanoparticle modified nano-sized liposomes. Dox loaded versions of these nanoparticles were shown to enhance drug release under induced hyperthermia (43°C). Confocal microscopy and flow cytometry analysis revealed CD44 targeted internalization of liposome nanoparticles in glioblastoma (U87 cells) tumor cells with a dual effect i.e. magneto-thermal and chemotherapeutic triggered the killing of tumor cells *in vitro*, suggesting their potential role as next-generation *in vivo* anti-cancer nano-vehicles [49].

4. Immunogenicity of HA-based nanoparticles

The extent of interaction between nanoparticles and serum proteins, i.e. the formation of the protein corona, is a key factor deciding the intravenous delivery efficiency of the nanoparticles. The protein corona may be modified using coatings that alter the surface properties of the nanoparticles. Almalik et al. showed that modifying chitosan NPs with HA avoided inflammatory protein adsorption compared to nanoparticles not coated with HA [50]. Similarly, reactive oxygen species (ROS) production was suppressed when activated macrophages were treated with HA modified chitosan nanoparticles. The secretion of cytokines such as TNF- α and IL-1 β were drastically reduced, indicating low immunogenicity of the HA-CS NPs without any collateral biological responses [51]. Zaki et al. also demonstrated that HA-chitosan NPs were taken up at a relatively slower rate compared to NPs not coated with HA. Moreover, the extent of internalization was two-fold lesser [52]. Further studies are required to verify that HA coatings decrease the immunogenicity of particulates.

5. Conclusions

Research in the development of active cancer-targeting agents led to the discovery of various cell surface molecules that control cellular function via different signaling pathways. CD44 is a cell surface protein that plays a significant role in tumorigenesis, metastasis, and proliferation of cancer cells. Several studies have demonstrated that the interaction of CD44 and HA, an extracellular component,

leads to the progression, growth, and metastasis of cancer cells via different signaling pathways. Consequently, strategies have been developed to fabricate HA mediated tumor targeting nanoplatforms. Moreover, it has been reported that conjugation of HA with different nanoparticles increases the internalization of therapeutic molecules via enhanced permeability and retention or CD44 mediated endocytosis with increased therapeutic efficacy both *in vivo* and *in vitro*. Particularly, various drug loaded targeting strategies have emerged, including redox, thermosensitive, and pH sensitive self-assembled HA-prodrug delivery and HA modified metallic and non-metallic nanovehicle-mediated delivery. In summary, HA-based nanoliposomes, micelles, and nano-carriers are promising therapeutic platforms for the delivery of multifunctional cargo in the context of active targeted cancer therapy, paving the way for next-generation clinical cancer therapy.

Acknowledgements

Dr. Nilkamal Pramanik acknowledges DST, SERB- DST (NPDF), Govt. of India, for their financial support.

Conflicts of interest

No conflict of interest is declared.

Author details

Nilkamal Pramanik* and Sameer Kumar Jagirdar
Centre for BioSystems Science and Engineering, Indian Institute of Science,
Bengaluru, Karnataka, India

*Address all correspondence to: nilkamalorganic@gmail.com

IntechOpen

© 2021 The Author(s). Licensee IntechOpen. This chapter is distributed under the terms of the Creative Commons Attribution License (<http://creativecommons.org/licenses/by/3.0>), which permits unrestricted use, distribution, and reproduction in any medium, provided the original work is properly cited. 

References

- [1] Han HS, Choi KY, KoH, et al. Bioreducible core-crosslinked hyaluronic acid micelle for targeted cancer therapy. *J Control Release*. 2015; 200:158-166. DOI: 10.1016/j.jconrel.2014.12.032.
- [2] Choi KY, Min KH, Yoon HY, et al. PEGylation of hyaluronic acid nanoparticles improves tumor targetability in vivo. *Biomaterials*. 2011; 32:1880-1889. Doi: 10.1016/j.biomaterials.2010.11.010.
- [3] Delmage, JM, Powars, DR, Jaynes, PK, Allerton, SE. The selective suppression of immunogenicity by hyaluronic acid. *Ann Clin Lab Sci*. 1986; 16(4):303-310.
- [4] Prajapati, VD, Maheriya, PM. Hyaluronic acid as potential carrier in biomedical and drug delivery applications. In: Maiti S, Jana S. Editors. *Functional Polysaccharides for Biomedical Applications*. 1st ed. Woodhead Publishing. Elsevier, 2019. p. 213-265. Doi.org/10.1016/B978-0-08-102555-0.00007-8.
- [5] Huang G, Huang H. Application of hyaluronic acid as carriers in drug delivery. *Drug Delivery*. 2018; 25: 766-772. Doi: 10.1080/10717544.2018.1450910..
- [6] Lee H, Lee K, Park TG. Hyaluronic acid-paclitaxel conjugate micelles: synthesis, characterization, and anti-tumor activity. *Bioconjugate Chem*. 2008; 19: 1319-1325. Doi: 10.1021/bc8000485.
- [7] Klingbeil P, Natrajan R, Everitt G, et al. CD44 is overexpressed in basal-like breast cancers but is not a driver of 11p13 amplification. *Breast Cancer Res Treat*. 2010; 120: 95-109. Doi.org/10.1007/s10549-009-0380-7.
- [8] Lakshman M, Subramaniam V, Rubenthiran U, et al. CD44 promotes resistance to apoptosis in human colon cancer cells. *Exp Mol Pathol*. 2004; 77: 18-25. DOI: 10.1016/j.yexmp.2004.03.002.
- [9] Ranuncolo SM, Ladedo V, Specterman S, et al. CD44 expression in human gliomas. *J Surg Oncol*. 2002; 79: 30-36. DOI: 10.1002/jso.10045.
- [10] Lukyanov, AN, Elbayoumi, TA, Chakilam, AR, Torchilin, VP. Tumor-targeted liposomes: doxorubicin-loaded long-circulating liposomes modified with anti-cancer antibody. *J. Controlled Release*. 2004; 100: 135-144. DOI: 10.1016/j.jconrel.2004.08.007.
- [11] Datir SR, Das M, Singh RP, et al. Hyaluronate tethered, "smart" multiwalled carbon nanotubes for tumor-targeted delivery of doxorubicin. *Bioconjugate Chem*. 2012; 23: 2201-2213. Doi.org/10.1021/bc300248t.
- [12] Yin, T, Liu, J, Zhao, Z, Zhao Y, Dong, L, Yang, M, Zhou J, and Huo, M. Redox Sensitive Hyaluronic Acid-Decorated Graphene Oxide for Photothermally Controlled Tumor-Cytoplasm-Selective Rapid Drug Delivery. *Adv. Funct. Mater*. 2017; 27: 1604620. Doi.org/10.1002/adfm.201604620.
- [13] Cai J, Fu J, Li R, Zhang, F, Ling G, Zhang, P. A potential carrier for anti-tumor targeted delivery-hyaluronic acid Nanoparticles. *Carbohydrate Polymers*. 2019; 208: 356-364. DOI:10.1016/j.carbpol.2018.12.074.
- [14] Meyer K, Palmer JW: The polysaccharide of the vitreous humor. *J Biol Chem* 1934; 107: 629-634.
- [15] Nagabhushan M, Pretlow TG, Guo YJ, et al. Altered expression of CD44 in human prostate cancer during progression. *Am J Clin Pathol*. 1996; 106: 647-651. Doi.org/10.1093/ajcp/106.5.647.

- [16] Wang SJ, Wong G, De Heer AM, et al. CD44 variant isoforms in head and neck squamous cell carcinoma progression. *Laryngoscope*. 2009; 119: 1518-1530. Doi: 10.1002/lary.20506.
- [17] Sugiyama M, Woodman A, Sugino T, et al. Non-invasive detection of bladder cancer by identification of abnormal CD44 proteins in exfoliated cancer cells in urine. *Clin Mol Pathol*. 1995; 48: 142-147. Doi: 10.1136/mp.48.3.m142.
- [18] Ponta H, Sherman L, Herrlich PA. CD44: From adhesion molecules to signalling regulators. *Nat. Rev. Cell Biol*. 2003; 4: 33-45. Doi.org/10.1038/nrm1004.
- [19] Sze JH, Brownlie JC, Love CA. Biotechnological production of hyaluronic acid: a mini review. *3Biotech*. 2016; 6:67. DOI: 10.1007/s13205-016-0379-9.
- [20] Chong BF, Blank LM, Mclaughlin R, Nielsen, LK. Microbial hyaluronic acid production. *Applied Microbiology and Biotechnology*. 2005; 66, 341-351. DOI:10.1007/s00253-004-1774-4.
- [21] Mao Z, Chen RR: Recombinant synthesis of hyaluronan by *Agrobacterium* sp. *Biotechnol Prog* 2007; 23:1038-1042. Doi: 10.1021/bp070113n.
- [22] Yu HM, Stephanopoulos G: Metabolic engineering of *Escherichia coli* for biosynthesis of hyaluronic acid. *Metabolic Eng* 2008; 10:24-32. DOI:10.1016/jymben.2007.09.001.
- [23] Sheng JZ, Ling PX, Zhu XQ, Guo XP, Zhang TM, He YL, Wang FS: Use of induction promoters to regulate hyaluronan synthase and UDP-glucose-6-dehydrogenase of *Streptococcus zooepidemicus* expression in *Lactococcus lactis*: a case study of the regulation mechanism of hyaluronic acid polymer. *J Appl Microbiol*. 2009; 107: 136-144. Doi. org/10.1111/j.1365-2672.2009.04185.x.
- [24] Lu, X, Kamat, MN, Huang, L, Huang, X. Chemical Synthesis of a Hyaluronic Acid Decasaccharide. *J Org Chem*. 2009; 74(20): 7608-7617. Doi: 10.1021/jo9016925.
- [25] Schante, CE, Zubera, G, Herlinb, C, Vandamme, TF. Chemical modifications of hyaluronic acid for the synthesis of derivatives for a broad range of biomedical applications. *Carbohydrate Polymers*. 2011; 85: 469-489. Doi. org/10.1016/j.carbpol.2011.03.019.
- [26] Yin, T, Wang J, Yin L, Shen L, Zhou J, Huo, M. Redox-sensitive hyaluronic acid-paclitaxel conjugates micelles with high physical drug loading for efficient tumor therapy. *Polym. Chem*. 2015; 6: 8047. DOI:10.1039/C5PY01355K.
- [27] Auzenne E, Ghosh SC, Khodadadian M, Rivera B, Farquhar D, Price RE, Ravoori M, Kundra V, Freedman RS, Klostergaard J. Hyaluronic acid-paclitaxel: anti-tumor efficacy against CD44(+) human ovarian carcinoma xenografts. *Neoplasia*. 2007; 9: 479-486. Doi:10.1593/neo.07229.
- [28] Rosato A, Banzato A, Luca GD, Renier D, Bettella F, Pagano C, Esposito G, Zanovello P, Bassi P. HYTAD1-p20: a new paclitaxel-hyaluronic acid hydrosoluble bioconjugate for treatment of superficial bladder cancer. *Urol. Oncol.-Semin. Original Invest*. 2006; 24: 207-215. Doi.org/10.1016/j.urolonc.2005.08.020.
- [29] Liao J, Zheng H, Fei Z, Lu B, Zheng H, Li D, Xiong X, Yi Y. Tumor-targeting and pH-responsive nanoparticles from hyaluronic acid for the enhanced delivery of doxorubicin. *International Journal of Biological Macromolecules*. 2018; 113: 737-747. DOI:10.1016/j.ijbiomac.2018.03.004.

- [30] Li WH, Yi X, Liu X., Zhang Z., Fu Y, & Gong T. Hyaluronic acid ion pairing nanoparticles for targeted tumor therapy. *Journal of Controlled Release*. 2016; 225: 170-182. Doi.org/10.1016/j.jconrel.2016.01.049.
- [31] Ling X, Zhao C, Huang L, Wang Q, Tu J, Shen Y, Sun C. Synthesis and characterization of hyaluronic acid-platinum (IV) nanoconjugate with enhanced antitumor response and reduced adverse effects. *RSC Adv*. 2015; 5: 81668. Doi.org/10.1039/C5RA16757D.
- [32] Li J, MeirongHuo M, Wang J, Zhou J, Mohammad JM, Zhang Y, Zhu Q, Waddad AY, Zhang Q. Redox-sensitive micelles self-assembled from amphiphilic hyaluronic aciddeoxycholic acid conjugates for targeted intracellular delivery of paclitaxel. *Biomaterials*. 2012; 33: 2310-2320. Doi: 10.1016/j.biomaterials.2011.11.022.
- [33] Deng L, Wang G, Ren J, Zhang B, Yan J, Li W, Khashab NM. Enzymatically triggered multifunctional delivery system based on hyaluronic acid micelles. *RSC Advances*. 2012; 2: 12909-12914. DOI: 10.1039/C2RA21888G.
- [34] Liu X, Li W, Chen T, Yang Q, Huang T, Fu Y, Gong T, Zhang Z. Hyaluronic acid modified micelles encapsulating Gem-C12 and HNK for glioblastoma multiforme chemotherapy. DOI: 10.1021/acs.molpharmaceut.7b01035.
- [35] Gao S, Wang J, Tian R, Wang G, Zhang L, Li Y, Li L, Ma Q, Zhu L. Construction and Evaluation of a Targeted Hyaluronic Acid Nanoparticle/Photosensitizer Complex for Cancer Photodynamic Therapy. *ACS Appl. Mater. Interfaces*. 2017; 9(38): 32509-32519. Doi.org/10.1021/acsami.7b09331.
- [36] Liu X, Li W, Chen T, Yang Q, Huang T, Fu Y, Gong T, Zhang Z. Hyaluronic Acid-Modified Micelles Encapsulating Gem-C12 and HNK for Glioblastoma Multiforme Chemotherapy. *Mol. Pharmaceutics*. 2018; 15: 1203-1214. Doi.org/10.1021/acs.molpharmaceut.7b01035.
- [37] Sun Y, Li X, Zhang L, Liu X, Jiang B, Long Z, Jiang Y. Cell Permeable NBD Peptide-Modified Liposomes by Hyaluronic Acid Coating for the Synergistic Targeted Therapy of Metastatic Inflammatory Breast Cancer. *Mol. Pharmaceutics*. 2019; 16: 1140-1155. DOI: 10.1021/acs.molpharmaceut.8b01123.
- [38] Fong Y T, Chen C H, Chen J P. Intratumoral delivery of doxorubicin on folate-conjugated graphene oxide by in-situ forming thermo-sensitive hydrogel for breast cancer therapy. *Nanomaterials*. 2017; 7:388-411. Doi: 10.3390/nano7110388.
- [39] Xu K, Lee F, Gao S J, Chung J E, Yano H, Kurisawa M. Injectable hyaluronic acid-tyramine hydrogels incorporating interferon- α 2a for liver cancer therapy. *Journal of Controlled Release*. 2013; 166: 203-210. Doi.org/10.1016/j.jconrel.2013.01.008.
- [40] Ashwinkumar N, Maya S, Jayakumar R. Redox-responsive cystamine conjugated chitin-hyaluronic acid composite nanogels. *RSC Adv*. 2014; 4: 49547. Doi.org/10.1039/C4RA06578F.
- [41] Luo Y, Cai X, Li H, Lin Y, Du D. Hyaluronic Acid-Modified Multifunctional Q-Graphene for Targeted Killing of Drug-Resistant Lung Cancer Cells. *ACS Applied Materials & Interfaces*. 2016; 8(6): 4048-4055. DOI: 10.1021/acsami.5b11471.
- [42] Jung H S, Kong W H, Sung D K, Lee M Y, Beack S E, Keum D H, Kim K S, Yun S H, Hahn S K. Nanographene Oxide Hyaluronic Acid Conjugate for Photothermal Ablation Therapy of Skin Cancer. *ACS Nano*. 2014; 8(1): 260-268. Doi.org/10.1021/nn405383a.

- [43] Pramanik N, Ranganathan S, Rao S, Suneet K, Jain S, Rangarajan A, Siddharth Jhunjhunwala, S. A Composite of Hyaluronic Acid-Modified Graphene Oxide and Iron Oxide Nanoparticles for Targeted Drug Delivery and Magnetothermal Therapy. *ACS Omega*. 2019; 4(5): 9284-9293. Doi: [org/10.1021/acsomega.9b00870](https://doi.org/10.1021/acsomega.9b00870).
- [44] Yu M, Jambhrunkar S, Thorn P, Chen J, Gu W, Yu C. Hyaluronic acid modified mesoporous silica nanoparticles for targeted drug delivery to CD44 over-expressing cancer cells. *Nanoscale*. 2013; 5: 178-183. Doi: [org/10.1039/C2NR32145A](https://doi.org/10.1039/C2NR32145A).
- [45] Palanikumar L, Kim J, Oh JY, Choi H, Park MP, Kim C, Ryu JH. Hyaluronic Acid-Modified Polymeric Gatekeepers on Biodegradable Mesoporous Silica Nanoparticles for Targeted Cancer Therapy. *ACS Biomater. Sci. Eng.* 2018; 4(5): 1716-1722. Doi: [org/10.1021/acsbiomaterials.8b00218](https://doi.org/10.1021/acsbiomaterials.8b00218).
- [46] Kang SH; Nafiujjaman M; Nurunnabi M, Li L; Khan HA, Cho KJ, Huh KM; Lee YK. Hybrid photoactive nanomaterial composed of gold nanoparticles, pheophorbide-A and hyaluronic acid as a targeted bimodal phototherapy. *Macromol. Res.* 2015; 23: 474-484. Doi: [org/10.1007/s13233-015-3061-x](https://doi.org/10.1007/s13233-015-3061-x).
- [47] Wang R, Luo Y, Yang S, Lin J, Gao D, Zhao Y, Liu J, Shi X, Wang X. Hyaluronic acid-modified manganese-chelated dendrimer-entrapped gold nanoparticles for the targeted CT/MR dual-mode imaging of hepatocellular carcinoma. *Sci. Rep.* 2016; 6: 1-10. DOI: [10.1038/srep33844](https://doi.org/10.1038/srep33844).
- [48] Luo, Y, Li Y, Li J, Fu C, Yu X, Wu L. Hyaluronic acid-mediated multifunctional iron oxide-based MRI nanoprobes for dynamic monitoring of pancreatic cancer. *RSC Adv.*, 2019; 9: 10486-10493. <https://doi.org/10.1039/C9RA00730J>.
- [49] Jose G, Lu YJ, Chen HA, Hsu HL, Hung JT, Anilkumar T.S, Chen JP. Hyaluronic acid modified bubble generating magnetic liposomes for targeted delivery of doxorubicin, *Journal of Magnetism and Magnetic Materials*. 2019; 474: 355-364. Doi: [org/10.1016/j.jmmm.2018.11.019](https://doi.org/10.1016/j.jmmm.2018.11.019).
- [50] Almalik A, Benabdelkamel H, Masood A, Alanazi IO, Alradwan I, Majrashi MA, Alfadda AA, Alghamdi WM, Alrabiah H, Tirelli N, Alhasan AH. Hyaluronic Acid Coated Chitosan Nanoparticles Reduced the Immunogenicity of the Formed Protein Corona. *Scientific Reports*. 2017; 7: 10542. Doi: [org/10.1038/s41598-017-10836-7](https://doi.org/10.1038/s41598-017-10836-7).
- [51] Almalik A, Alradwan I, Majrashi MA, Alsaffar BA, Algarni AT, Alsuabeyl MS, Alrabiah H, Tirelli N, Alhasan AH. Cellular Responses of Hyaluronic Acid Coated-Chitosan Nanoparticles. *Toxicol. Res.* 2018; 7: 942-950. DOI: [10.1039/C8TX00041G](https://doi.org/10.1039/C8TX00041G).
- [52] Zaki NM, Nasti A, Tirelli N. Nanocarriers for Cytoplasmic Delivery: Cellular Uptake and Intracellular Fate of Chitosan and Hyaluronic Acid-Coated Chitosan Nanoparticles in a Phagocytic Cell Model. *Macromol. Biosci.* 2011; 11: 1747-1760. Doi: [10.1002/mabi.201100156](https://doi.org/10.1002/mabi.201100156).